Elastic and Inelastic Light–Matter Interactions in 2D Materials

Jiajie Pei, Jiong Yang, and Yuerui Lu

(Invited Paper)

***Abstract*—Two-dimensional (2D) materials such as graphene, transition metal dichalcogenides and phosphorene have emerged as brand new photonic materials with huge potential in a variety of optical applications in recent years, due to their unique properties and multiple functions. Owning to the significantly increased surface to volume ratio in the atomic thin layered structure, the interactions between 2D materials with light become remarkably strong in either elastic or inelastic interactions. Most of previous studies were focused on the inelastic interactions between 2D materials with light, namely Raman and photoluminescence properties. However, we found the elastic interactions between them and light are also very attractive. Based on the properties discovered, we demonstrated several optical applications, such as atomically thin optical lenses and gratings. On the other hand, we found the inelastic interactions with light in the 2D limitation affected a lot by the external environment, which could serve as a unique method to control the working status of the optical devices to meet multiple application needs. Several progresses were demonstrated such as control of excitons and trions in few-layer MoS_2 via the co-modulations by both temperature and electric field and the defect engineering by oxygen plasma etching to stimulate new photon emission.**

***Index Terms*—2D materials, defect, exciton, gratings, lens, plasma etching, trion.**

I. Introduction

SINCE the discovery of graphene and its astonishing properties, a new class of materials known as "2D materials", such as transition metal dichalcogenide semiconductors (TMDs), phosphorene, h-BN and layered metal oxides, have attracted tremendous attentions owing to their unique properties and sensitivity to the external environment. Among which, the optical properties such as strong interactions with light [1]–[3], layer-dependent energy gaps [4], [5], tunable exciton dynamics [6], [7], and tightly bound trions [8], [9], etc, make them promising candidates for various optical devices and optoelectronic devices. The fundamental mechanisms of these devices are based on the interactions between light and 2D materials. There are two categories interactions between light and matter: inelastic and elastic [10]. An inelastic interaction involves energy transfer between photons and electrons or phonons. In contrast, elastic interactions do not involve energy transfer, and are responsible for controlling the propagation of light.

Optical components, such as resonant cavities, waveguides, lenses, gratings, optical meta-materials [11] and photonic crystals [12], all rely on strong elastic interactions between light and matter to achieve sophisticated control of the flow of light. Strong elastic interactions rely on significant changes of the amplitude and phase of the light accumulated over a long optical path. Thus, for the atomically thin materials, such as a single layer graphene sheet, the interaction is normally very small [13]. Much efforts has been done to this issue, but only plasmonic resonance in graphene can enhance the elastic optical response in the mid- to far-infrared range [14]–[16]. It is still a great challenge to control the flow of light using 2D materials in the visible and near-infrared regions, where most interesting optoelectronic properties exist. Surprisingly, the strength of the elastic interaction in a 2D material increases dramatically with the increase of refractive index. Such favorable scaling makes high-index 2D TMD semiconductors [17], [18] particularly attractive for the application of strong elastic light–matter interactions.

On the other hand, the inelastic interaction of light involves energy transfer between photons–electrons or photons–phonons, which result in the photoluminescence (PL) phenomenon and Raman effect, respectively. Optical devices such as LED, transistors and solar cells, are working relying on the interaction between photons and electrons. The electronic band structure of a semiconductor material plays a key role in the interaction process. Thus, the band structure investigation and modulation become of great importance in the design of optical devices. For 2D materials, the band structures are more sensitive to the external environment due to the significantly increased surface to volume ratio compared with their bulk form and therefore could be easily controlled by the corresponding techniques [19]–[21]. In other words, the inelastic light-matter interactions become more complicated if the status of surrounding environment changes. As a result, the optical properties of 2D materials could totally change. For instance, the PL spectrum of MoS_2 strongly depends on the layer number and layer-stacking sequences [22]–[24]. Particularly, monolayer TMDs have the most distinct properties compared with their few-layer counterpart due to the absence of interlayer interactions and reduced screening effect [25]. For few-layer TMDs, interlayer interaction, screening effect, quantum confinement and crystal symmetry jointly determine their electronic structures [1],

Manuscript received April 24, 2016; accepted May 21, 2016. This work was supported in part by the ANU Ph.D. student scholarship, China Scholarship Council, National Natural Science Foundation of China under Grant 11162014, in part by the Australian Research Council, and in part by the ANU Major Equipment Committee.

J. Pei is with the School of Mechanical Engineering, Beijing Institute of Technology, Beijing, 100081, China, and also with the NEMS Laboratory, Research School of Engineering, Australian National University, Canberra, ACT 2601, Australia (e-mail: jiajie.pei@gmail.com).

J. Yang and Y. Lu are with the NEMS Laboratory, Research School of Engineering, Australian National University, Canberra, ACT 2601, Australia (e-mail: jiong.yang@anu.edu.au; yuerui.lu@anu.edu.au).

Color versions of one or more of the figures in this paper are available online at http://ieeexplore.ieee.org.

Digital Object Identifier 10.1109/JSTQE.2016.2574599

[22]–[24]. Especially, phosphorene is always a direct bandgap semiconductor in each layer number while the bandgap ranging from mid-infrared to near-infrared wavelengths. Owning to the sensitivity of the inelastic interactions between light and 2D materials, many works could be done to investigate the evolution of their optical properties as a function of the change or stimulation in surrounding environment, such as van der Waals interactions, temperature, electric field, magnetic field, strains and surface defects, which may enable the possibility of discovering more unique phenomena in 2D materials and developing a variety of novel optical applications.

In this paper, we discuss the recent progress on the properties of 2D materials and their applications in optical devices based on both the elastic and inelastic interactions between light and 2D materials. Section II illustrates the remarkably high index and optical path length (OPL) of MoS_2 and their applications in atomically thin optical lenses and gratings. Comparisons have been made between our results and other groups' recent progresses. Future improvement possibilities on these devices were discussed. Section III gives a brief summary on the research interests on the inelastic interactions between light and 2D materials. Several potential research directions were discussed based on the demonstration of two representative recent findings by our group, regarding the modulations of inelastic interactions between light and 2D materials by external stimulation method. One is the control of excitons and trions dynamic in few-layer MoS_2 via the co-modulations by both temperature and electric field. The other one is the defect engineering technique through layer-by-layer thinning of thick exfoliated phosphorene flakes using oxygen plasma etching.

II. *Elastic Light–Matter Interactions*

To characterize the elastic interaction between light and matter, one possible method is to measure its phase shift when light propagates the material. And by making use of the optical interferometry, the phase shift can be measured with a phase-shifting interferometer (PSI). Previously Venkatachalam *et al.* have reported to use such technique to measure the phase shift of thin-layer graphene and the layer number of thin-layer graphene can be accurately determined down the thickness of monolayer [26]. They have also reported an optical thickness of about 2 nm for single layer of graphene, which is within expectation considering the fact that the physical thickness of single layer of graphene is only about 0.35 nm. The refractive optical components reply on the OPL to modify the phase front of an optical beam, and the OPL is directly related to the geometrical length of light path. As a result, it is normally expected that thin-layer 2D materials would be too thin to generate a large OPL value, as shown in thin-layer graphene, and thus the phase front cannot be modified efficiently in such ultra-thin materials. However, an OPL value of 38 nm has been observed from monolayer molybdenum disulphide (MoS_2) with the PSI system [27]. During the measurements, the OPL value of monolayer MoS_2 on SiO_2/Si substrate was defined as $OPL_{MoS_2} = -\frac{\lambda}{2\pi}(\phi_{MoS_2} - \phi_{SiO_2})$, where λ is the wavelength of the light source and it is 535 nm in the experiment, ϕ_{MoS_2} and ϕ_{SiO_2} are the PSI measured phase shifts of thelight reflected from the MoS_2 flake and the SiO_2/Si substrate (Fig. 1(a) inset), respectively. The giant OPL value of monolayer MoS_2 is more than 50 times larger comparing with its physical thickness of 0.67 nm and it is one order of amplitude larger than its counterpart from monolayer graphene. Interestingly, comparable OPL values have also been observed in other monolayer TMD semiconductors, about 40 nm for monolayer WS_2 and WSe_2 [27], and a OPL value of around 20 nm have also been observed in monolayer phosphorene [28].

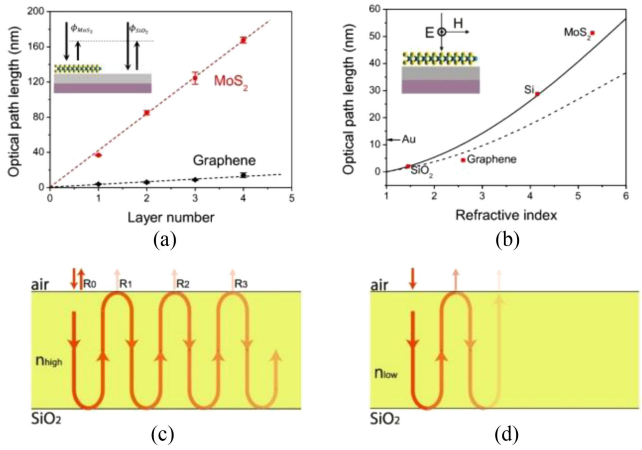

Fig. 1. High refractive index enabled giant OPL in ultra-thin film. (a) Statistical data of the OPL values from PSI for 1–4 L MoS_2 and graphene samples. Inset is the schematic plot showing the PSI measured phase shifts of the reflected light from the MoS_2 flake and the SiO_2 substrate. (b) Simulated OPL values for light reflected from 2D material (0.67 nm in thickness) with different indices on a SiO_2 (275 nm)/Si substrate (solid line) and SiO_2 substrate with infinite thickness (dashed line). (c)–(d) Schematic plots of multiple reflections at the interfaces of ultra-thin 2D materials. Figure reproduced from [27].

The underling physics of such giant OPL value from monolayer MoS_2 lies in its high refractive index. At 535 nm, the wavelength of the light source used in the PSI system, the refractive indices of monolayer MoS_2 and graphene is $4.4 + 0.6i$ and $2.6 + 1.3i$, respectively [29], [30]. Theoretical simulation indicates that the OPL value is highly related to the refractive index value, and it will increase rapidly with the increase of materials' refractive indices (Fig. 1(b)). This correlation between OPL values and refractive index can be explained by the schematic plots shown in Fig. 1(c) and (d). When the thin-layer material owns a high refractive index (the same case as monolayer MoS_2), the large impedance mismatch at MoS_2-air and MoS_2-SiO_2 interfaces will lead to large reflection coefficients at those interfaces, resulting in multiple reflections inside the high refractive index material (Fig. 1(c)). These multiple reflections will significantly enhance the geometrical length of light path within the monolayer MoS_2, which generates the giant OPL value. On the contrary, if the thin-layer material owns a low refractive index (the same case as monolayer graphene), the impedance mismatch in the interfaces will be low, leading to less reflections within the material and a small OPL value (Fig. 1(d)).

A. *MoS_2 Lenses*

Based on experimental results, the OPL value of thin layer MoS_2 will increase by more than 50 nm with the layer thickness increasing by 1 nm [27]. With the giant OPL from thin-layer

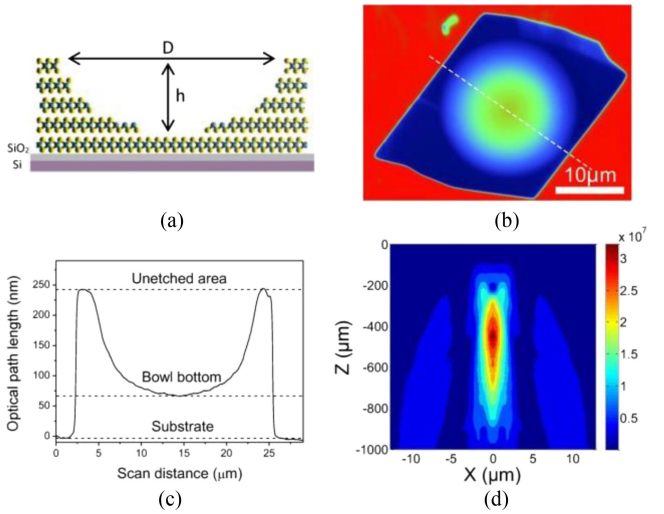

Fig. 2. Atomically thin micro-lens fabricated from a few-layers of MoS_2. (a) Schematic plot of the micro-lens structure. (b) PSI image of an atomically thin micro-lens fabricated on a 9 L MoS_2 flake. (c) Measured OPL values versus position for the direction indicated by the dashed line in (b). (d) Intensity distribution pattern of the MoS_2 micro-lens measured by scanning optical microscopy (SOM). Figure reproduced from [27].

MoS_2, the phase front can be efficiently controlled with only atomically thin structure. By making use of such property to engineer the phase front of an optical beam, a refractive concave lens has been fabricated with only a few atomic layers of MoS_2 (Fig. 2(a) and (b)). The fabrication process starts with a uniform nine-layer MoS_2 flake, and it is milled to the pre-designed bowl-shape lens by focused ion beam (FIB). The bowl-shape profile is clearly shown from the PSI measurements (Fig. 2(c)). From the measured profile of the micro-lens, its focal length is calculated to be 248 μm. In order to characterize the fabricated MoS_2 micro-lens, the light path of a micro-Raman system was modified to be a far-field scanning optical microscope (SOM). The SOM system used a green laser (at 532 nm) as the light source, consistent with the wavelength used in simulations. By moving the micro-lens along the z-axis insteps of 10 μm by a piezo-electrically driven stage, the camera recorded a series of the intensity distributions with the MoS_2 micro-lens positioned at different z values. A 3D dataset was then generated by data processing and a cross section profile was obtained along the x- and z-axes to illustrate the average distribution of the light intensity in these directions (Fig. 2(d)). The focal length f of the MoS_2 micro-lens was measured to be 240 μm.

We have also noticed other works of ultra-thin lenses based on different materials. Kim *et al.* reported self-assembled nanoscale spherical lenses based on organic materials CHQ with near-field focusing and magnification capabilities. [32] Fattal *et al.* reported flat dielectric reflectors with focusing abilities based on amorphous silicon. [33] And recently, Gu *et al.* have also reported ultra-thin lenses with 3D subwavelength focusing based on graphene oxide. [34] By comparing the above mentioned three typical ultra-thin lenses with our micro-lens based on few-layer MoS_2, we have generated Table I consisting of lens parameters and performances. It can be clear seen that our MoS_2 micro-lens can outperform other ultra-thin lenses in aspects such as thickness and numerical aperture (NA) value. And by further improving its NA value and focusing efficiency, the MoS_2 micro-lens will be more capable for future optical systems.

TABLE I
COMPARISON BETWEEN DIFFERENT ULTRA-THIN LENSES

Lens	Thickness	NA	Focusing efficiency
Nanoscale CHQ spherical lens [32]	$<$800 nm	–	–
Flat amorphous silicon lens [33]	~450 nm	~0.01	80–90%[a]
Ultra-thin graphene oxide lens [34]	~200 nm	–	$>$32%
MoS2 micro-lens [27]	~6.3 nm	~0.2	–

[a] This value is the total reflection.

With focal length of 240 μm, lens diameter of 20 μm and the lens material refractive index of 4.4, a simple calculation shows that the NA of this micro-lens based on few-layer of MoS_2 is ~0.2 by using equation $NA \approx \frac{n \cdot D}{2f}$, where n is the refractive index of the medium in which the lens is working, D is the lens diameter and f is the focal length of the lens. This NA value of the micro-lens needs to be further improved for application as ultra-thin optical elements. Several approaches can be considered, including electrically tuning the refractive index of thin-layer MoS_2 as indicated in Ref [31] and redesign the lens structure to achieve higher $\frac{D}{f}$ ratio.

B. MoS_2 Gratings

Light scattering is another elastic interaction between light and matter. Devices that employ photonic band gap [35], Anderson localization [36], and light trapping such as with thin-film solar cells [37] all rely heavily on strong light scattering. And the elastic interaction can be quantified by measuring the scattering efficiency. Theoretical simulation shows that the scattering cross section is highly dependent on the refractive index of materials (Fig. 3(a)). Required by the boundary condition of Maxwell's equations, the electrical field inside a 2D material is almost as strong as the tangential component of the incident field, leading to a strong polarization $P = \varepsilon_0(n^2 - 1)E_0$, where E_0 is the electric field of s-polarized incident light, n is the index of the material and ε_0 is the electric permittivity of free space. The scattering power is proportional to the P^2 and, therefore, scales roughly as n^4, as shown by the dash trend line in Fig. 3(a). This scaling rule greatly favors high-index materials and is again uniquely available in ultra-thin materials.

Grating fabricated from few-layer MoS_2 flakes with FIB is schematically shown in Fig. 3(b). The atomic force microscope (AFM) images of gratings made from mono-, bi- and eight-layer MoS_2 are shown in Fig. 3(c) and (d). The grating parameters, including periodicity and filling ratio, are calculated for each layer for optimal configuration. The gratings are characterized with 532 nm green laser, consistent with the light source wavelength used in simulation. First and second order diffraction can be observed during experiments and the diffraction efficiency is calculated based on measured results. The measured maximum diffraction efficiency for grating made from 1 L, 2 L, 6 L and 8 L gratings are 0.3%, 0.8%, 4.4% and 10.1%, respectively. As a comparison, no diffracted beam can be observed from the grating fabricated from CVD grown monolayer graphene, con-

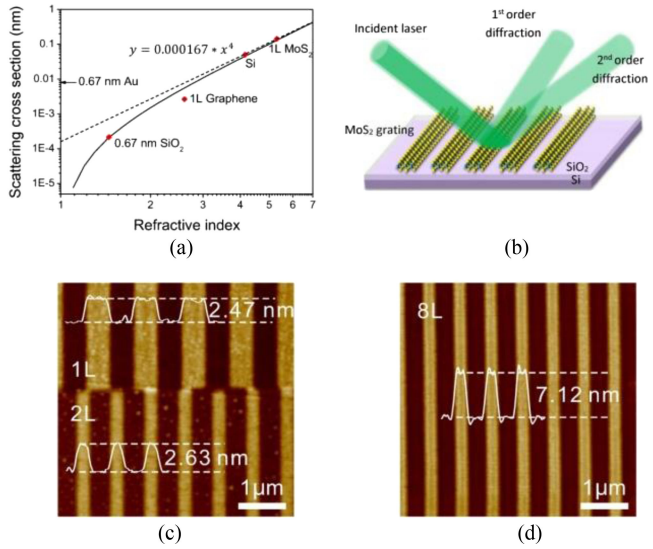

Fig. 3. Atomically thin high-efficiency gratings made from single- and few-layer MoS_2. (a) Simulated scattering cross section (SCS) versus refractive index for a layer of 0.67 nm thick material. The dashed line is added as a reference. (b) Schematic of grating and diffraction efficiency measurement setup. (c–d) AFM images of 1 L, 2 L and 8 L MoS_2 gratings. Figure reproduced from [27].

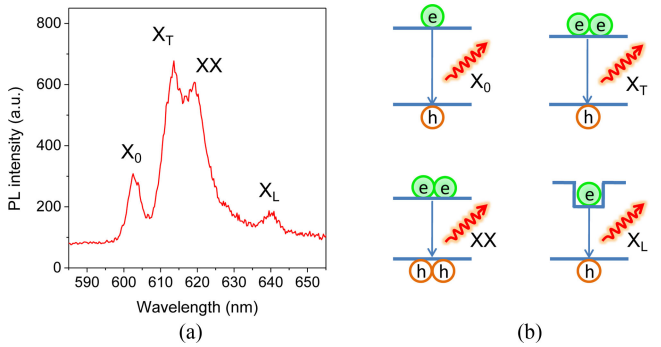

Fig. 4. Typical Photoluminescence emission features of monolayer 2D materials. (a) PL spectrum of monolayer WS_2 at 77 K. X_0 represents exciton; X_T represents trion; X_X represents biexciton; X_L represents localized exciton. (b) Schematic of the photon emission processes from exciton, trion, biexciton and localized exciton. "e" stands for electrons; "h" stands for holes. It should be noted that the trion could be constituted by two electrons with a hole (negative trion), or by two holes with an electron (positive trion).

firming that the scattering efficiency is highly dependent on the refractive index.

By replacing the Si substrate used in our experiment with a metallic mirror, the diffraction efficiency of MoS_2 gratings can be further improved. Theoretical simulation indicates that with optical design, the 1st order grating diffraction efficiency of an 8 L MoS_2 grating can be up to 23.7%. In addition, an asymmetrical profile as used in high-efficiency gratings is expected to further improve the efficiency. Besides, by making use of materials' high refractive index and the resulting high scattering efficiency, this periodic structure fabricated from thin-layer MoS_2 can be further utilized as Bragg reflectors as shown in Ref. [38].

III. Inelastic Light–Matter Interactions

The inelastic light–matter interaction normally implies the PL and Raman effects, which involves energy transfer between photons–electrons and photons–phonons, respectively. Therefore, the Raman phenomenon is affected by the lattice structure of a material and can be used to characterize the quality or status of the crystal, whereas the PL phenomenon is highly related to the bandgap of a semiconductor and is the basis of the development of novel optical devices. In the field of 2D materials, the groundbreaking material, graphene, has zero bandgap at its pristine status that would limit its applications in optical devices, although its bandgap could be induced by the external stimulation. In contrast, the recently discovered TMDs and phosphorene naturally have adequate bandgap values ranging from visible to near-infrared wavelengths that make them more suitable for the development of novel optical devices.

Due to the significantly reduced screening effect in the 2D limit, the TMDs undergo a gradual transition from an indirect bandgap in bulk to a direct bandgap in their monolayer form that strongly enhance their PL emission. At the same time, the quasi-particle binding energies increase a lot in the 2D nanosheet, which makes the PL spectra not only contains the exciton (combination of one electron and one hole) emission, but also enables the emerging of other many-body effect such as trion (combination of one electron and two holes or two electrons and one hole), biexciton (combination of two electrons and two holes) and localized exciton (defect emission). Fig. 4 shows a typical PL of 2D materials that contains abovementioned four features. These features may not be easy to show up at the same time (affected by temperature or doping). The many-body effect in 2D materials such as carrier multiplication and Wigner crystallization [39] has recently aroused much attention of researchers but most of previous studies and findings are limited to monolayers [5], [7], [8]. However, the few-layer structures are also important, since the interlayer van der Waals interactions would affect the light–matter interactions and trigger new fundamental phenomena that can enable many new optical devices based on heterostuctures [40]. Besides the van der Waals interactions, many other external mediums such as temperature, electric field, magnetic field, strains and surface defects could also have significant impacts on the interactions between light and 2D materials due to the large surface to volume ratio in the atomically thin layers, which could probably stimulate several unique phenomenon and enable a variety of novel optical applications.

A. Trion dynamics With van der Waals Interactions

Trion is a charged exciton that has an extra electron/hole with nonzero spin, which is a very important composition in the PL spectra of 2D materials that can be used for spin manipulation [41], [42] and it offers remarkable optoelectronic applications [43]–[47]. The previous study found that the exciton and trion dynamics in monolayer MoS_2 could be tuned by up to two orders of magnitude by electric field at room temperature [7], [8] owing to the direct bandgap. However, the PL spectra in bilayer MoS_2 could not be tuned by electric field at room temperature due to its indirect bandgap [6] arising from the interlayer van

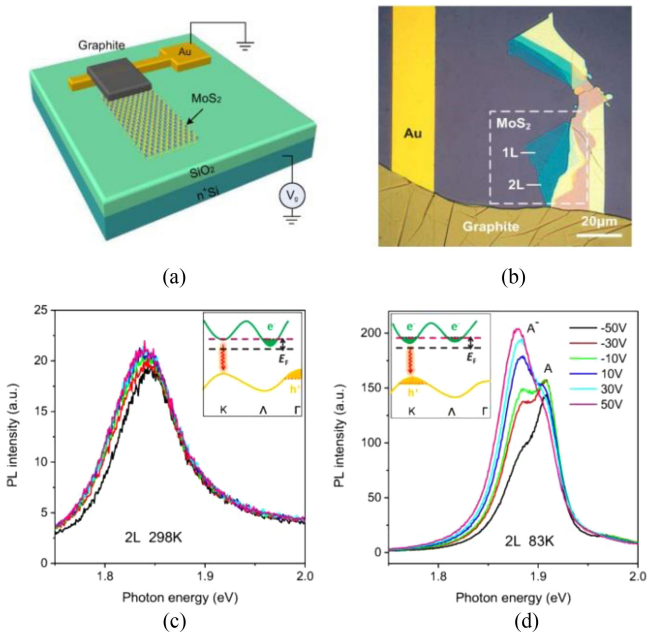

Fig. 5. MoS_2 metal-oxide-semiconductor (MOS) device and the PL of bilayer MoS_2 by both temperature and electric field modulation. (a–b) Schematic plot and optical microscope image of the MoS_2 MOS device. (c–d) Measured PL spectra from 2 L MoS_2 sample, under different back gate voltages (from −50 to 50 V) and at temperature of 298 K and 83 K, respectively. Insets show the schematic plots of the corresponding band structures with indicated quasi-Fermi level. Figure reproduced from [48].

der Waals interactions. Through the theoretical calculation we found that as temperature decreases from 300 to 100 K, the Λ valley of the conduction band moves down relatively to the K valley in monolayer MoS_2, while the Λ valley rises up relatively to the K valley in bilayer MoS_2. The evolution of band structure at different temperatures would enable different photocarrier relaxation pathways in mono- and bi-layer of MoS_2. Since the band structure of 2D material is sensitive to temperature, we cooled down the bilayer MoS_2 to 83 K and found that the PL intensity increased by around one order of magnitude which is very similar with the phenomenon arising from indirect to direct bandgap transition. As a result, the exciton and trion dynamics in bilayer MoS_2 became tunable again at low temperature [48].

A back-gated metal-oxide-semiconductor (MOS) device was used (Fig. 5(a) and (b)) to apply electric field in the experiment. Mono- and bi-layer MoS_2 was mechanically exfoliated and drily transferred [49] onto a SiO_2/Si substrate near a pre-patterned gold electrode, followed by another thick graphite flake bridging the gold electrode and MoS_2 flake, forming a MOS device. In the experiment, the gold electrode is grounded, and the Si substrate functions as a back gate (Fig. 5(a)). In the experiment, we swinged the back gate voltage from −50 to 50 V. For the monolayer MoS_2, the same excitons and trions dynamics were observed as previous study [8]. However, in the bilayer MoS_2, we did not observe gate tunable PL spectra at room temperature (Fig. 5(c)), whereas when the temperature went down to 83 K, the gate dependent exciton and trion dynamics became obvious (Fig. 5(d)), which could be explained as follows:

At 298 K, owning to the van der Waals interactions, bilayer MoS_2 has an indirect band gap and the Femi level E_F locates near the Λ valley. The electric field could only tune the photoelectron density within the Λ valley instead of within the K valley (Fig. 5(c) inset). Since the main PL peak comes from the direct K-K transition, the electric field cannot affect the main PL emission at room temperature. This situation changes at 83 K when the Λ valley moves up and the K valley moves down relatively that the weight of photoelectrons relaxed to K valley was highly enhanced. And the Femi level E_F locates near the K valley now which enables the tunability of photoelectron density within the K valley (Fig. 5(d) inset). As a result, the exciton and trion dynamics could be tuned in bilayer MoS_2 at 83 K. Moreover, due to the opposite valley movements in mono- and bilayer MoS_2 as a function of temperature, the PL intensity of bilayer MoS_2 increase twice faster than that of monolayer MoS_2 and finally surpassed it at 83 K.

These findings provide insight into exciton and trion dynamics with van der Waals interactions in multilayer 2D materials and have possibility to enable new applications in photonics and optoelectronics [1], [2], [50]. And the co-modulation by both electric field and temperature provides a novel method to investigate the fundamental phenomena in other few-layer 2D materials. It should be noted that although the TMDs have the same lattice structure and similar band structures, they optical properties are not always similar, some could be totally opposite, such as the temperature dependent PL intensities from bilayer MoS_2 and $MoSe_2$ [51]. Moreover, even for the same material, the multi-layers can exhibit totally different properties from the monolayer just because of the van der Waals interactions. Therefore, in the future, research of multi-layer 2D materials is necessary, since it can not only help us gain more understanding of the light–matter interactions in 2D materials, but also provides opportunities to develop novel optical devices based on multi-layer 2D materials.

B. Low-Dimensional Excitons in Defect States

Defects in semiconductors can strongly influence electric and optical properties of the device and such interactions become stronger in 2D materials due to the tighter localization of the electron wave function [52]. Structural defects, such as vacancies, dislocations and interstitials are commonly observed in both exfoliated and grown TMDs [53], [54]. It is true that these defects can strongly influence the inelastic light–matter interactions, but not all of them are disadvantageous if we can take full advantage of them. For example, PL emission can be strongly enhanced in MoS_2 through defect engineering [55]. Understanding the functionalities of defects, and the ability to precisely control them, can improve the performance of 2D materials and has potential to lead to new applications [56].

Many works have been done on the investigation of defects in 2D TMD materials and several interesting results have been reported [53]–[57]. However, for the recently developed 2D material, phosphorene, rare research has been done on the influence of defects. Particularly, phosphorene has quasi-1D excitonic nature [58], [59], layer-dependent direct bandgap [60], [61] and anisotropic nature [62]–[67]. These properties contrast

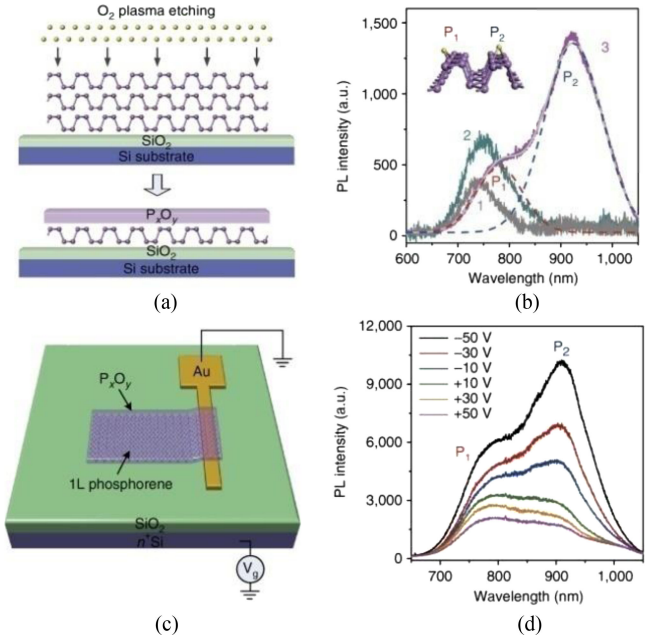

Fig. 6. Oxygen defect engineering in stabilized monolayer phosphorene. (a) Schematic showing the oxygen plasma etching technique. (b) Measured PL spectra of monolayer phosphorene samples produced by different methods: 1–exfoliated; 2–fabricated by oxygen plasma etching; 3–fabricated by oxygen plasma etching with defect engineering. Inset is schematic plot of two different oxygen defects in monolayer phosphorene (P_1–horizontal bridge and P_2–diagonal bridge). (c) Schematic plot of the monolayer phosphorene MOS structure and the electrical measurement setup. (d) Measured PL spectra from the defect engineered monolayer phosphorene, under different back gate voltages from −50 to +50 V. Figure reproduced from [72].

dramatically with other 2D materials, such as graphene [68] and TMD semiconductors [8], [69], [70]. Phosphorene could therefore provide a unique platform to investigate the dynamics of excitons in reduced dimensions and fundamental many-body interactions [28], [58], [71] with surface defects.

In our recent research, we found that oxygen plasma etching technique could not only be used to thin down the phosphorene thick flakes layer by layer (Fig. 6(a)), but also offer the opportunity to introduce defect states in a stabilized phosphorene monolayer [72]. Interestingly, when the sample was thinned down to monolayer and over-etched a little, a brand new PL emission status appeared in the spectrum at room temperature, compared with the PL spectrum of exfoliated monolayer phosphorene (Fig. 6(b)). The O_2 plasma etching fabricated monolayer phosphorene shows one PL emission peak at 750 nm, which is the same with that from a mechanically exfoliated phosphorene monolayer. This 750-nm-peak is denoted as the trion peak of a pristine monolayer phosphorene in our previous research [28]. When the oxygen defects have been introduced into the monolayer phosphorene, two strong PL peaks at 780 and 915 nm show in the spectrum, whereas the 750-nm-peak was significantly diminished and the 915-nm-peak has much higher PL intensity than the intrinsic trion emission. Moreover, the defect-induced PL emission can be further modulated by electric field using a MOS-structure device (Fig. 6(c) and (d)), which could lead to new applications like electrically tunable and broadband lighting source in the NIR range at room temperature.

TABLE II
COMPARISON OF DEFECTS EMISSIONS IN TMDS AND PHOSPHORENE

2D materials	Showing temperatures	Localization energies
MoS_2	Cryogenic temperature	0.12 eV
$MoSe_2$	Cryogenic temperature	0.23 eV
WSe_2	Cryogenic temperature	0.11 eV
Phosphorene	Room temperature	0.18 & 0.42 eV

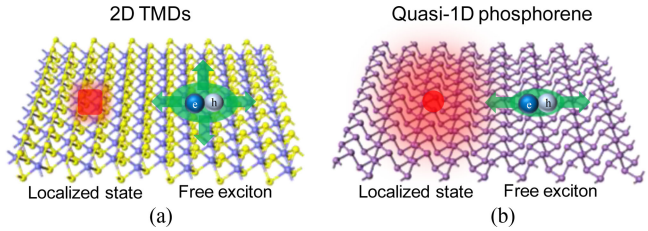

Fig. 7. Schematic of exciton diffusion and localization in 2D TMDs and quasi-1D phosphorene. (a) A free exciton in TMDs diffuses along the 2D plane and has little possibility to meet the localized state and emits PL. (b) A free exciton in monolayer phosphorene diffuses along the armchair axis and converts to a 0D exciton at the localized state and emits brighter PL.

According to the previous numerical simulations [73], these two peaks could be attributed to the localized excitons that induced by oxygen atoms bridging across the phosphorene atoms. There are two types of oxygen bridging defects: diagonal bridge and horizontal bridge with positive binding energies that may be formed when the oxygen source is more reactive than the O_2 ground state, for example, under light pumping or O_2 plasma. For a diagonal bridge defect, the oxygen atom connects phosphorus atoms on different edges of the zigzag ridge. For a horizontal bridge defect, the oxygen atom connects the phosphorus atoms from the same edge (as illustrated in Fig. 6(a) inset). Both types of surface bridge defects are expected to create levels in the bandgap and are able to give rise to recombination lines in luminescence experiments [73].

The localized exciton emissions in phosphorene is quite unique, since for monolayer TMD semiconductors such emissions can only be seen at cryogenic temperatures [56]. While the oxygen defects induced exciton localization could be clearly observed in a monolayer phosphorene at room temperature, and the localization energy is much larger than that in TMDs (see Table II, the values of TMDs are extracted from Ref. [56]). One of the reasons could be because of the large trapping energy in phosphorene [73]. The other reason could be the quasi-1D excitonic nature of monolayer phosphorene. In the quasi-1D space, the rapid collision between excitons and local quencher states can significantly limit the luminescence quantum yield of free excitons [58], [59]. Conversely, the defect states act as 0D photoluminescent centers instead of acting as exciton quenchers that can capture mobile excitons and convert them into photons in very high luminescence quantum yield. Therefore, the intrinsic 1D excitons [74], [75] are diminished and the localized 0D excitons become more brightening than the intrinsic limit (as illustrated in Fig. 7(b)). Whereas in the 2D TMDs, the free excitons are less limited by the quencher states and

therefore can diffuse along the 2D plane that has little possibility to meet the localized state and emits photons. On the other hand, the quantum yield of 1D excitons could be reduced by the temperature-limited radiative decay rate at high temperature. While the temperature-independent radiative decay rate of 0D excitons is free from this restriction. This could lead to the emerging of localized excitons emissions at room temperature and a remarkable enhancement of the quantum yield for 0D excitons. In addition, it is found that the lifetimes of localized excitons are significantly longer than that of free excitons. This may be due to the highly reduced non-radiative decay rate resulting from the localization effect of squeezing an exciton in the 0D state [75], [76]. The longer lifetime would benefit to the performance of photonic devices such as light oscillators and photonic crystals.

This suggests that the localized excitons in monolayer phosphorene could serve as a unique platform to explore the fundamental inelastic light–matter interactions in a 2D–1D–0D hybrid system and open up new avenues for the development of novel optical devices.

IV. Conclusion

In this paper, we classified the recent findings on optical properties and devices of 2D materials into two categories: elastic and inelastic interactions between light and 2D materials. We revealed the unique elastic and inelastic interactions between light and 2D materials based on our recently proposed applications such as atomically thin optical lenses and gratings, valley control of excitons and trions and defect engineering technique. Similar research progresses by other groups were compared and discussed. Future perspectives on these directions were addressed.

At last, it is worth emphasizing that due to the significantly increased surface to volume ratio in the 2D form, the light-2D materials interactions could be modulated in a large scale by the external media such as temperature, electric field, magnetic field, strains, acoustic wave, etc. Any coupling between light with the other medium could probably stimulate several unique properties that makes the 2D materials quite exciting and having huge potential in a variety of optical applications like tunable light sources, photo-detectors, sensors and spin manipulation devices.

References

[1] L. Britnell *et al.*, "Strong light-matter interactions in heterostructures of atomically thin films," *Science*, vol. 340, pp. 1311–1314, Jun. 14, 2013.

[2] G. Eda and S. A. Maier, "Two-dimensional crystals: Managing light for optoelectronics," *ACS Nano*, vol. 7, pp. 5660–5665, Jul. 23, 2013.

[3] M.-L. Tsai *et al.*, "Monolayer MoS_2 heterojunction solar cells," *ACS Nano*, vol. 8, pp. 8317–8322, Aug. 26, 2014.

[4] J. K. Ellis, M. J. Lucero, and G. E. Scuseria, "The indirect to direct band gap transition in multilayered MoS_2 as predicted by screened hybrid density functional theory," *Appl. Phys. Lett.*, vol. 99, 2011, Art. no. 261908.

[5] A. Splendiani *et al.*, "Emerging photoluminescence in monolayer MoS_2," *Nano Lett.*, vol. 10, pp. 1271–1275, Apr. 14, 2010.

[6] A. K. M. Newaz *et al.*, "Electrical control of optical properties of monolayer MoS_2," *Solid State Commun.*, vol. 155, pp. 49–52, 2013.

[7] J. S. Ross *et al.*, "Electrically tunable excitonic light-emitting diodes based on monolayer WSe_2 p-n junctions," *Nature Nano*, vol. 9, pp. 268–272, 2014.

[8] K. F. Mak *et al.*, "Tightly bound trions in monolayer MoS_2," *Nature Mater.*, vol. 12, pp. 207–211, 2013.

[9] T. C. Berkelbach, M. S. Hybertsen, and D. R. Reichman, "Theory of neutral and charged excitons in monolayer transition metal dichalcogenides," *Phys. Rev. B*, vol. 88, Jul. 25, 2013, Art. no. 045318.

[10] J. Weiner and P.-T. Ho, Light-Matter Interaction, Fundamentals and Applications, vol. 1, New York, NY, USA: Wiley, 2003.

[11] N. Engheta and R. W. Ziolkowski, Metamaterials: Physics and Engineering Explorations. New York, NY, USA: Wiley, 2006.

[12] J. D. Joannopoulos, S. G. Johnson, J. N. Winn, and R. D. Meade, Photonic Crystals: Molding the Flow of Light, 2nd ed. Princeton, NJ, USA: Princeton Univ. Press, 2008.

[13] F. Bonaccorso, Z. Sun, T. Hasan, and A. C. Ferrari, "Graphene photonics and optoelectronics," *Nature Photon.*, vol. 4, pp. 611–622, 2010.

[14] S. H. Lee *et al.*, "Switching terahertz waves with gate-controlled active graphene metamaterials," *Nature Mater.*, vol. 11, pp. 936–941, 2012.

[15] L. Ju *et al.*, "Graphene plasmonics for tunable terahertz metamaterials," *Nature Nanotechnol.*, vol. 6, pp. 630–634, 2011.

[16] A. Vakil and N. Engheta, "Transformation optics using graphene," *Science*, vol. 332, pp. 1291–1294, 2011.

[17] B. Radisavljevic, A. Radenovic, J. Brivio, V. Giacometti, and A. Kis, "Single-layer MoS_2 transistors," *Nature Nanotechnol.*, vol. 6, pp. 147–150, 2011.

[18] C.-C. Shen, Y.-T. Hsu, L.-J. Li, and H.-L. Liu, "Charge dynamics and electronic structures of monolayer mos_2 films grown by chemical vapor deposition," *Appl. Phys. Exp.*, vol. 6, 2013, Art. no. 125801.

[19] R. Xu *et al.*, "Exciton brightening in monolayer phosphorene via dimensionality modification," *Adv. Mater.*, vol. 28, pp. 3493–3498, 2016.

[20] R. Xu *et al.*, "Layer-dependent surface potential of phosphorene and anisotropic/layer-dependent charge transfer in phosphorene-gold hybrid systems," *Nanoscale*, vol. 8, pp. 129–135, 2016.

[21] Z. Yi *et al.*, "Strongly enhanced photoluminescence in nanostructured monolayer MoS_2 by chemical vapor deposition," *Nanotechnology*, vol. 27, 2016, Art. no. 135706.

[22] Q. H. Wang, K. Kalantar-Zadeh, A. Kis, J. N. Coleman, and M. S. Strano, "Electronics and optoelectronics of two-dimensional transition metal dichalcogenides," *Nature Nano*, vol. 7, pp. 699–712, 2012.

[23] X. Yin *et al.*, "Edge nonlinear optics on a MoS_2 atomic monolayer," *Science*, vol. 344, pp. 488–490, May 2, 2014.

[24] K. F. Mak, K. He, J. Shan, and T. F. Heinz, "Control of valley polarization in monolayer MoS_2 by optical helicity," *Nature Nano*, vol. 7, pp. 494–498, 2012.

[25] T. Cheiwchanchamnangij and W. R. L. Lambrecht, "Quasiparticle band structure calculation of monolayer, bilayer, and bulk MoS_2," *Phys. Rev. B*, vol. 85, 2012, Art. no. 205302.

[26] D. K. Venkatachalam, P. Parkinson, S. Ruffell, and R. G. Elliman, "Rapid, substrate-independent thickness determination of large area graphene layers," *Appl. Phys. Lett.*, vol. 99, 2011, Art. no. 234106.

[27] J. Yang *et al.*, "Atomically thin optical lenses and gratings," *Light Sci. Appl.*, vol. 5, 2016, Art. no. e16046.

[28] J. Yang *et al.*, "Optical tuning of exciton and trion emissions in monolayer phosphorene," *Light Sci. Appl.*, vol. 4, 2015, Art. no. e312.

[29] H. Zhang *et al.*, "Measuring the refractive index of highly crystalline monolayer MoS_2 with high confidence," *Sci. Rep.*, vol. 5, 2015, Art. no. 8440.

[30] P. Blake *et al.*, "Making graphene visible," *Appl. Phys. Lett.*, vol. 91, 2007, Art. no. 063124.

[31] E. J. G. Santos and E. Kaxiras, "Electrically driven tuning of the dielectric constant in MoS_2 layers," *ACS Nano*, vol. 7, pp. 10741–10746, Dec. 23, 2013.

[32] J. Y. Lee *et al.*, "Near-field focusing and magnification through self-assembled nanoscale spherical lenses," *Nature*, vol. 460, pp. 498–501, 2009.

[33] D. Fattal, J. Li, Z. Peng, M. Fiorentino, and R. G. Beausoleil, "Flat dielectric grating reflectors with focusing abilities," *Nature Photon.*, vol. 4, pp. 466–470, 2010.

[34] X. Zheng *et al.*, "Highly efficient and ultra-broadband graphene oxide ultrathin lenses with three-dimensional subwavelength focusing," *Nature Commun.*, vol. 6, 2015, Art. no. 8433.

[35] E. Yablonovitch, "Inhibited spontaneous emission in solid-state physics and electronics," *Phys. Rev. Lett.*, vol. 58, pp. 2059–2062, 1987.

[36] S. John, "Strong localization of photons in certain disordered dielectric superlattices," *Phys. Rev. Lett.*, vol. 58, pp. 2486–2489, 1987.

[37] Z. Yu, A. Raman, and S. Fan, "Thermodynamic upper bound on broadband light coupling with photonic structures," *Phys. Rev. Lett.*, vol. 109, 2012, Art. no. 173901.

[38] Y. Jiang *et al.*, "Porous silicon omnidirectional Bragg reflector for Si solar cells," presented at the Light Energy Environment, Canberra, Australia, 2014, Paper PW2B.1.

[39] E. Wigner, "On the interaction of electrons in metals," *Phys. Rev.*, vol. 46, pp. 1002–1011, 12/01/ 1934.

[40] A. K. Geim and I. V. Grigorieva, "Van der Waals heterostructures," *Nature*, vol. 499, pp. 419–425, 07/25/print 2013.

[41] C. Galland and A. Imamoğlu, "All-optical manipulation of electron spins in carbon-nanotube quantum dots," *Phys. Rev. Lett.*, vol. 101, 10/08/2008, Art. no. 157404.

[42] X. Xu, W. Yao, D. Xiao, and T. F. Heinz, "Spin and pseudospins in layered transition metal dichalcogenides," *Nature Phys.*, vol. 10, pp. 343–350, 2014.

[43] V. I. Klimov *et al.*, "Optical gain and stimulated emission in nanocrystal quantum dots," *Science*, vol. 290, pp. 314–317, Oct. 13, 2000.

[44] S. G. Carter *et al.*, "Quantum coherence in an optical modulator," *Science*, vol. 310, pp. 651–653, Oct. 28, 2005.

[45] G. D. Scholes and G. Rumbles, "Excitons in nanoscale systems," *Nature Mater.*, vol. 5, pp. 683–696, 2006.

[46] A. A. High, E. E. Novitskaya, L. V. Butov, M. Hanson, and A. C. Gossard, "Control of exciton fluxes in an excitonic integrated circuit," *Science*, vol. 321, pp. 229–231, July 11, 2008.

[47] K. Kheng *et al.*, "Observation of negatively charged excitons in semiconductor quantum wells," *Phys. Rev. Lett.*, vol. 71, pp. 1752–1755, 1993.

[48] J. Pei *et al.*, "Exciton and trion dynamics in bilayer MoS_2," *Small*, vol. 11, pp. 6384–6390, 2015.

[49] A. Castellanos-Gomez *et al.*, "Deterministic transfer of two-dimensional materials by all-dry viscoelastic stamping," *2D Mater.*, vol. 1, 2014, Art. no. 011002.

[50] D. Kozawa *et al.*, "Photocarrier relaxation pathway in two-dimensional semiconducting transition metal dichalcogenides," *Nature Commun.*, vol. 5, 2014, Art. no. 4543.

[51] S. Tongay *et al.*, "Thermally driven crossover from indirect toward direct bandgap in 2D semiconductors: $MoSe_2$ versus MoS_2," *Nano Lett.*, vol. 12, pp. 5576–80, Nov 14, 2012.

[52] X. L. Yang, S. H. Guo, F. T. Chan, K. W. Wong, and W. Y. Ching, "Analytic solution of a two-dimensional hydrogen atom. I. Nonrelativistic theory," *Phys. Rev. A*, vol. 43, pp. 1186–1196, 1991.

[53] H. Qiu *et al.*, "Hopping transport through defect-induced localized states in molybdenum disulphide," *Nature Commun.*, vol. 4, 2013, Art. no. 2742.

[54] W. Zhou *et al.*, "Intrinsic structural defects in monolayer molybdenum disulfide," *Nano Lett.*, vol. 13, pp. 2615–22, Jun 12, 2013.

[55] H. Nan *et al.*, "Strong photoluminescence enhancement of MoS_2 through defect engineering and oxygen bonding," *ACS Nano*, vol. 8, pp. 5738–5745, 2014.

[56] S. Tongay *et al.*, "Defects activated photoluminescence in two-dimensional semiconductors: interplay between bound, charged, and free excitons," *Sci. Rep.*, vol. 3, 2013, Art. no. 2657.

[57] H.-P. Komsa *et al.*, "Two-dimensional transition metal dichalcogenides under electron irradiation: defect production and doping," *Phys. Rev. Lett.*, vol. 109, 2012, Art. no. 035503.

[58] V. Tran, R. Soklaski, Y. Liang, and L. Yang, "Layer-controlled band gap and anisotropic excitons in few-layer black phosphorus," *Phys. Rev. B*, vol. 89, 2014, Art. no. 235319.

[59] R. Xu *et al.*, "Extraordinarily bound quasi-one-dimensional trions in two-dimensional phosphorene atomic semiconductors," *ACS Nano*, vol. 10, pp. 2046–2053, 2016.

[60] J. Qiao, X. Kong, Z.-X. Hu, F. Yang, and W. Ji, "High-mobility transport anisotropy and linear dichroism in few-layer black phosphorus," *Nature Commun.*, vol. 5, 2014, Art. no. 4475.

[61] S. Zhang *et al.*, "Extraordinary photoluminescence and strong temperature/angle-dependent raman responses in few-layer phosphorene," *ACS Nano*, vol. 8, pp. 9590–9596, 2014.

[62] H. Liu *et al.*, "Phosphorene: An unexplored 2D semiconductor with a high hole mobility," *ACS Nano*, vol. 8, pp. 4033–4041, 2014.

[63] M. Buscema *et al.*, "Fast and broadband photoresponse of few-layer black phosphorus field-effect transistors," *Nano Lett.*, vol. 14, pp. 3347–3352, 2014.

[64] R. Fei and L. Yang, "Strain-engineering the anisotropic electrical conductance of few-layer black phosphorus," *Nano Lett.*, vol. 14, pp. 2884–2889, 2014.

[65] F. Xia, H. Wang, and Y. Jia, "Rediscovering black phosphorus as an anisotropic layered material for optoelectronics and electronics," *Nature Commun.*, vol. 5, 2014, Art. no. 4458.

[66] L. Li *et al.*, "Black phosphorus field-effect transistors," *Nature Nano*, vol. 9, pp. 372–377, 2014.

[67] T. Hong *et al.*, "Polarized photocurrent response in black phosphorus field-effect transistors," *Nanoscale*, vol. 6, pp. 8978–8983, 2014.

[68] A. K. Geim and K. S. Novoselov, "The rise of graphene," *Nature Mater.*, vol. 6, pp. 183–191, 2007.

[69] B. Radisavljevic, A. Radenovic, J. Brivio, V. Giacometti, and A. Kis, "Single-layer MoS_2 transistors," *Nature Nano*, vol. 6, pp. 147–150, 2011.

[70] J. Yang *et al.*, "Robust excitons and trions in monolayer $MoTe_2$," *ACS Nano*, vol. 9, pp. 6603–6609, 2015.

[71] A. S. Rodin, A. Carvalho, and A. H. Castro Neto, "Excitons in anisotropic two-dimensional semiconducting crystals," *Phys. Rev. B*, vol. 90, 2014, Art. no. 075429.

[72] J. Pei *et al.*, "Producing air-stable monolayers of phosphorene and their defect engineering," *Nature Commun.*, vol. 7, 2016, Art. no. 10450.

[73] A. Ziletti, A. Carvalho, D. K. Campbell, D. F. Coker, and A. H. Castro Neto, "Oxygen defects in phosphorene," *Phys. Rev. Lett.*, vol. 114, 2015, Art. no. 046801.

[74] S. Ghosh, S. M. Bachilo, R. A. Simonette, K. M. Beckingham, and R. B. Weisman, "Oxygen doping modifies near-infrared band gaps in fluorescent single-walled carbon nanotubes," *Science*, vol. 330, pp. 1656–1659, 2010.

[75] Y. Miyauchi *et al.*, "Brightening of excitons in carbon nanotubes on dimensionality modification," *Nature Photon*, vol. 7, pp. 715–719, 2013.

[76] H. Wang *et al.*, "Radiative lifetimes of excitons and trions in monolayers of the metal dichalcogenide MoS_2," *Phys. Rev. B*, vol. 93, 2016, Art. no. 045407.

Jiajie Pei received the Bachelor's degree in mechanical engineering from the Beijing Institute of Technology, Beijing, China. He received the Ph.D. degree from the Beijing Institute of Technology and Australia National University under the co-training. He is currently doing research in the NEMS Lab in Australian National University. His research interests include synthesis and characterization of 2D materials, design and fabrication of novel 2D materials devices.

Jiong Yang received the Bachelor's degree in materials sciences from the Fudan University, China, before moving to Australia. He is currently working toward the Ph.D. degree at the NEMS Lab, Australian National University. His Ph.D. project is on high-index induced properties of 2D materials and optical device fabrication and characterization based on such properties. His research interests include 2D materials, fabrication and characterization, nanolithography techniques and device design based on 2D materials.

Yuerui Lu received the Ph.D. degree from the Cornell University, the School of Electrical and Computer Engineering, in 2012. He received the B.S. degree from the Department of Applied Physics, University of Science and Technology of China, Hefei, China. In 2013, he joined the Australian National University as a Research Fellow and Lecturer under the Future Engineering Research Leadership Fellowship. In October 2015, he was promoted to Senior Lecturer at the ANU. Before that, he worked as a Postdoctoral Research Associate in SonicMEMS Laboratory, Cornell University. His research interests include MEMS/NEMS sensors and actuators, nano-manufacturing technologies, renewable energy harvesting, biomedical novel devices, nano-materials, nano-electronics, etc.